Transverse instability and its long-term development for solitary waves of the (2+1)-dimensional Boussinesq equation

Article (Published Version)

Transverse instability and its long-term development for solitary waves of the (2+1)-dimensional Boussinesq equation

K. B. Blyuss, T. J. Bridges, and G. Derks
Department of Mathematics & Statistics, University of Surrey, Guildford GU2 7XH, United Kingdom
(Received 23 August 2002; published 27 May 2003)

The stability properties of line solitary wave solutions of the $(2+1)$-dimensional Boussinesq equation with respect to transverse perturbations and their consequences are considered. A geometric condition arising from a multisymplectic formulation of this equation gives an explicit relation between the parameters for transverse instability when the transverse wave number is small. The Evans function is then computed explicitly, giving the eigenvalues for the transverse instability for all transverse wave numbers. To determine the nonlinear and long-time implications of the transverse instability, numerical simulations are performed using pseudospectral discretization. The numerics confirm the analytic results, and in all cases studied, the transverse instability leads to collapse.

DOI: 10.1103/PhysRevE.67.056626 PACS number(s): 05.45.Yv, 47.35.+i

I. INTRODUCTION

One of the fundamental ways that a solitary wave traveling in one space dimension generates a two-space-dimensional pattern is through transverse instability. A transverse instability of a line solitary wave is associated with a class of perturbations traveling in a direction transverse to the basic direction of propagation. In addition to establishing the existence of the transverse instability, a major question is what implications this instability has for the long-term behavior of the system: does it settle into a new two-space-dimensional pattern, or collapse? In this paper, we study this sequence of questions for the canonical Boussinesq equation in two space dimensions,

$$u_{tt}=(f(u)+\varepsilon u_{xx}))_{xx}+\sigma u_{yy}, \tag{1}$$

where $\varepsilon=\pm 1$ and $\sigma=\pm 1$. In general, $f(u)$ can be any smooth function, but the canonical form of the Boussinesq equation has the form

$$f(u)=D(u^2-u) \quad \text{with} \quad D=\pm 1.$$

When $D=-1$, $\varepsilon=1$, and $\sigma=1$, this equation was derived by Johnson [1] to describe the propagation of gravity waves on the surface of water, in particular, the head-on collision of oblique waves, and it was derived by Breizman and Malkin [2] in the context of Langmuir waves.

In the absence of the transverse variation (i.e., $u_y=0$) and for $\varepsilon=-1$, $D=-1$ this equation reduces to the so-called ''good'' Boussinesq equation, which is well posed, and for which sech^2 solutions exist for any c with $|c|<1$. These waves are stable when $\frac{1}{2}<|c|<1$ [3]. For the case $|c|<\frac{1}{2}$ it was shown by computer-assisted simulation of the leading term in the Taylor expansion of the Evans function that there is an unstable eigenvalue [4]. This result was generalized to include solitary waves with nonzero tails, and rigorously proved using the symplectic Evans matrix in Ref. [5].

The transverse instability of solitary waves has been widely studied since the seminal work of Zakharov [6] on the nonlinear Schrödinger equation and the work of Kadomtsev and Petviashvili [7] on the transverse instability of the Korteweg-de Vries soliton. Since then, the transverse instability of solitary waves has been investigated for a wide range of models; examples include the nonlinear Schrödinger (NLS) equation and related equations [8–10], the Kadomtsev-Petviashvili equation [11–14], the Zakharov-Kuznetsov equation [9,15,16], and water waves [17]. A review of the transverse instability for the NLS equation and other related models can be found in the work of Kivshar and Pelinovsky [14].

In this paper, we will first use a geometric condition as derived in Ref. [16] to get an explicit criterion for small transverse wave number instability. For this we use the multisymplectic formulation of Eq. (1) in an essential way. To get detailed information for all transverse wave numbers, we compute explicitly the Evans function for the $(2+1)$-dimensional Boussinesq model linearized about a larger family of line solitary waves (allowing the state at infinity to be nonzero). Plots of the dependence of the growth rate on the transverse wave number are presented.

The postinstability behavior of the nonlinear problem is studied using direct numerical simulation. The numerical evidence confirms the analytic results and suggests that the postinstability in the nonlinear system leads to collapse in all cases. A multisymplectic pseudospectral discretization [18] is used as a basis for the numerical simulations. The numerical scheme is applied to the full two-dimensional PDE and we observe transverse modulation and further development of the longitudinal and transverse instabilities, resulting in the collapse of the initial line solitary waves. In the parameter region where the analytic criterion indicates that the solitary wave state is longitudinally stable but transversely unstable, simulations support the analytic results and provide insight into the long-term development of this instability.

II. MULTISYMPLECTIFYING THE EQUATIONS

The Boussinesq system has a range of geometric structures. First, we record the Lagrangian and Hamiltonian structures. Let $u=\phi_{xx}$, then the system is Lagrangian with

$$L=\int\left[-\frac{1}{2}\phi_{xt}^2+F(\phi_{xx})+\frac{1}{2}\varepsilon\phi_{xxx}^2+\frac{1}{2}\sigma\phi_{xy}^2\right]dxdydt,$$

where $F(\cdot)$ is any function satisfying $F'(\cdot)=f(\cdot)$.

The Boussinesq equation can be represented as a Hamiltonian system in a number of ways (e.g., Ref. [19]). For example, let

$$H=\int\left[F(u)-\frac{1}{2}\varepsilon u_x^2+\frac{1}{2}\Phi_x^2+\frac{1}{2}\sigma w_y^2+\gamma(u-w_x)\right]dxdy, \tag{2}$$

where γ is a Lagrange multiplier associated with the constraint $u=w_x$. With Hamiltonian variables (Φ,u,w,γ), the governing equations take the form

$$\begin{aligned}-u_t&=\frac{\delta H}{\delta\Phi}=-\Phi_{xx},\\ \Phi_t&=\frac{\delta H}{\delta u}=f(u)+\varepsilon u_{xx}+\gamma,\\ 0&=\frac{\delta H}{\delta w}=\gamma_x-\sigma w_{yy},\\ 0&=\frac{\delta H}{\delta\gamma}=u-w_x.\end{aligned} \tag{3}$$

However, the most interesting form of Eq. (1) for the present purposes is the multisymplectic formulation, which can be represented in the canonical form [20]

$$\mathbf{M}Z_t+\mathbf{K}Z_x+\mathbf{L}Z_y=\nabla S(Z),\quad Z\in\mathbb{R}^6, \tag{4}$$

where

$$Z=\begin{pmatrix}q_1\\q_2\\q_3\\p_1\\p_2\\p_3\end{pmatrix},$$

$$\mathbf{M}=\begin{pmatrix}0&1&0&0&0&0\\-1&0&0&0&0&0\\0&0&0&0&0&0\\0&0&0&0&0&0\\0&0&0&0&0&0\\0&0&0&0&0&0\end{pmatrix}\quad\text{with}$$

$$u(x,y,t)=q_1(x,y,t),$$

$$\mathbf{K}=\begin{pmatrix}0&0&0&1&0&0\\0&0&0&0&1&0\\0&0&0&0&0&1\\-1&0&0&0&0&0\\0&-1&0&0&0&0\\0&0&-1&0&0&0\end{pmatrix},$$

$$\mathbf{L}=\begin{pmatrix}0&0&1&0&0&0\\0&0&0&0&0&0\\-1&0&0&0&0&0\\0&0&0&0&0&0\\0&0&0&0&0&0\\0&0&0&0&0&0\end{pmatrix},$$

$$S(Z)=-F(q_1)-\frac{1}{2\varepsilon}p_1^2+\frac{1}{2}p_2^2-\frac{\sigma}{2}p_3^2.$$

Using $q_1=u$ it is straightforward to show that this system is a reformulation of Eq. (1).

III. GEOMETRIC CRITERION FOR THE TRANSVERSE INSTABILITY

An advantage of the multisymplectic formulation is that there is a geometric condition which is easy to verify for the transverse instability of line solitary waves [16].

Consider the well-known basic family of solitary waves of Eq. (1) of the form

$$Z(x,y,t)=\hat{Z}(\theta;c,l),\quad \theta=x-ct+ly+\theta_0, \tag{5}$$

obtained by taking the first component to be a sech^2 wave,

$$u(\theta;c,l)=\langle\mathbf{e}_1,\hat{Z}(\theta;c,l)\rangle=A(c,l)\,\mathrm{sech}^2[B(c,l)\theta], \tag{6}$$

with

$$B(c,l)=\frac{1}{2}\sqrt{\varepsilon(D+c^2-\sigma l^2)},\quad A(c,l)=6\frac{\varepsilon}{D}B^2.$$

The existence of the solitary wave clearly requires $\varepsilon(D+c^2-\sigma l^2)>0$. The other components of $\hat{Z}$ are easily obtained from Eq. (6) and the multisymplectic equations (4).

For the linear stability analysis, let $Z(x,y,t)=\hat{Z}(\theta;c,l)+\mathrm{Re}[U(\theta;\lambda,k)e^{\lambda t+iky}]$, substitute this into Eq. (4) and linearize. Then, if the resulting linear equation has square-integrable solutions $U(\theta;\lambda,k)$ with $\mathrm{Re}(\lambda)>0$ and $k\in\mathbb{R}$, we call the basic solitary wave state $\hat{Z}(\theta;c,l)$ transversely unstable. Assuming that $\hat{Z}_\theta$ is the only square integrable element in the kernel of the linearization operator $\mathcal{L}=D^2S(Z)-[\mathbf{K}-c\mathbf{M}+l\mathbf{L}](d/d\theta)$, we have the following geometric condition of the transverse instability for small λ and k. Suppose

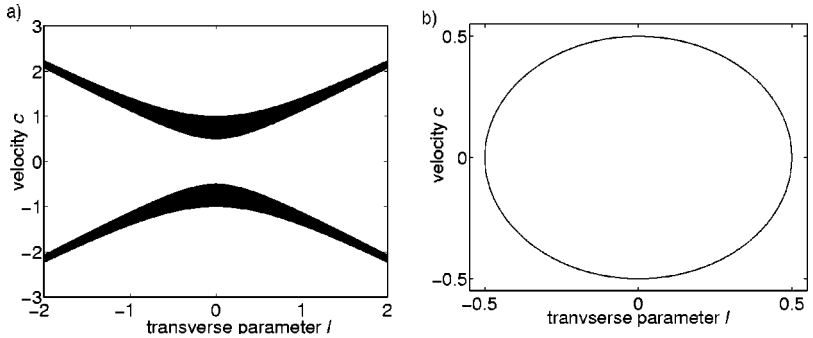

FIG. 1. Theoretical boundaries of the transverse instability for the ''good'' Boussinesq equation. (a) Case (14) with $\sigma=1$. The waves are unstable for the parameters lying within the shaded regions. (b) Case (15) with $\sigma=-1$. The waves are unstable for the parameters within the circle.

$$\Delta=\begin{vmatrix}\mathcal{A}_c & \mathcal{A}_l\\ \mathcal{B}_c & \mathcal{B}_l\end{vmatrix}>0, \quad \text{where} \quad \mathcal{A}=-\frac{1}{2}\int_{-\infty}^{\infty}\langle \mathbf{M}\hat{Z}_\theta,\hat{Z}\rangle d\theta,$$

$$\mathcal{B}=\frac{1}{2}\int_{-\infty}^{\infty}\langle \mathbf{L}\hat{Z}_\theta,\hat{Z}\rangle d\theta. \tag{7}$$

Then the basic solitary wave $\hat{Z}(\theta;c,l)$ of Eq. (1) is linearly transverse unstable [16,17].

Using the above definitions of the multisymplectic matrices **M** and **L**, we obtain

$$\mathcal{A}=-\frac{1}{2}\int_{-\infty}^{\infty}\left(q_1\frac{d}{d\theta}q_2-q_2\frac{d}{d\theta}q_1\right)d\theta=-c\int_{-\infty}^{\infty}q_1^2 d\theta$$

$$=-cK, \tag{8}$$

$$\mathcal{B}=\frac{1}{2}\int_{-\infty}^{\infty}\left(q_1\frac{d}{d\theta}q_3-q_3\frac{d}{d\theta}q_1\right)d\theta=\sigma l\int_{-\infty}^{\infty}q_1^2 d\theta=\sigma lK, \tag{9}$$

where

$$K=\int_{-\infty}^{\infty}u^2 d\theta=\frac{4}{3}\frac{A^2}{B}=-\frac{6\varepsilon}{D^2}(\sigma l^2-c^2-D)\sqrt{-\frac{\sigma l^2-c^2-D}{\varepsilon}}.$$

Substitution of Eqs. (8) and (9) in Eq. (7) yields

$$\begin{aligned}\operatorname{sgn}\Delta&=\operatorname{sgn}\left[-\frac{\sigma}{c}\mathcal{A}\left(\mathcal{A}_c+\frac{l}{c}\mathcal{A}_l\right)\right]\\&=\operatorname{sgn}\left[\sigma\left(\mathcal{A}_c+\frac{l}{c}\mathcal{A}_l\right)\right]\\&=\operatorname{sgn}\left[-\sigma\left(K+c\frac{\partial}{\partial c}K+l\frac{\partial}{\partial l}K\right)\right]\\&=\operatorname{sgn}[-\sigma(\sigma l^2-c^2-D)(4\sigma l^2-4c^2-D)].\end{aligned} \tag{10}$$

Since the condition for the transverse instability requires $\Delta>0$, we have the following result: *Suppose*

$$\varepsilon\sigma(4\sigma l^2-4c^2-D)>0, \tag{11}$$

then the basic solitary wave $\hat{Z}(\theta;c,l)$ *is linearly transversely unstable*.

The multisymplectic formulation also provides an expression for the linear growth rate of the instability λ as a function of the transverse wave number k for long-wave perturbations [16]:

$$\begin{aligned}\lambda&=\frac{\sqrt{\mathcal{A}_c\mathcal{B}_l-\mathcal{A}_l\mathcal{B}_c}}{|\mathcal{A}_c|}k+O(k^2)\\&=\frac{\sqrt{-\sigma(4\sigma l^2-4c^2+1)(\sigma l^2-c^2+1)}}{4c^2-1-\sigma l^2}k+O(k^2).\end{aligned} \tag{12}$$

This provides the growth rate for k small. In the following section, the Evans function will be constructed in order to determine the growth rate for all transverse wave numbers k.

In the remainder of this section, we apply condition (11) for various parameter values.

For the good Boussinesq equation from Ref. [3] with $\varepsilon=-1$ and $D=-1$ the existence and transverse instability requirements are

$$\sigma l^2-c^2+1>0 \quad \text{and} \quad -\sigma\left(\sigma l^2-c^2+\frac{1}{4}\right)>0, \tag{13}$$

respectively. Combining these conditions leads to the following system of inequalities for c and l when $\sigma>0$:

$$\tfrac{1}{4}+\sigma l^2<c^2<1+\sigma l^2, \tag{14}$$

and for $\sigma<0$

$$c^2<\tfrac{1}{4}+\sigma l^2. \tag{15}$$

These inequalities define the regions in (c,l) parameter plane, where the basic solitary wave exits and is linearly transversely unstable, and these regions are presented in Fig. 1.

One can do a similar analysis for Johnson's equation [1], where $\sigma=1$, $\varepsilon=1$, and $D=-1$. The existence requirement is $l^2<c^2-1$ and the instability condition is $l^2>c^2-\frac{1}{4}$. This

result is inconclusive for two reasons. First, the two regions do not overlap so the geometric condition does not predict instability for any parameter values. Second, when $\varepsilon=+1$ the equation is ill posed as an evolution equation (this can be seen at the linear level where the dispersion relation predicts instability as the wave number goes to infinity), and so the question of long-time stability is irrelevant.

IV. THE EVANS FUNCTION ANALYSIS OF THE TRANSVERSE INSTABILITY

In this section we use the Evans function formalism in order to analyze the linear transverse stability problem for the Boussinesq model (1) for all values of the transverse wave number. We restrict attention to the parameter values of most interest: $\varepsilon=-1$ and $D=-1$ associated with the good Boussinesq, although we put no restriction on σ (but keeping in mind that $\sigma=+1$ is the most interesting case).

However, the class of solitary waves will be enlarged. Namely, we include solitary waves biasymptotic to a nontrivial state at infinity, specifically,

$$U(\theta)=U_\infty+6\delta^2\ \mathrm{sech}^2(\delta\theta),\quad \theta=x-ct+ly, \tag{16}$$

where

$$\delta=\tfrac{1}{2}(\sqrt{1+4a}-c^2+\sigma l^2)^{1/2}\quad\text{and}\quad U_\infty=\tfrac{1}{2}(1-c^2+\sigma l^2)$$

$$-2\delta^2=-\frac{2a}{1+\sqrt{1+4a}}. \tag{17}$$

The value of the parameter a is constrained only by the existence of the square root: $1+4a\geqslant(c^2-\sigma l^2)^2$.

Here we will not use any geometric structure (although it might be interesting to look more closely in this direction) and so work directly with Eq. (1). Let

$$u(x,y,t)=U(\theta)+\mathrm{Re}\{\tilde{u}(\theta)\exp[iky+\lambda t]\}. \tag{18}$$

By substituting this expression in Eq. (1) and linearizing, one obtains the following equation for the complex function $\tilde{u}(\theta)$:

$$\tilde{u}_{\theta\theta\theta\theta}+2(U\tilde{u})_{\theta\theta}-(1-c^2+\sigma l^2)\tilde{u}_{\theta\theta}-2(c\lambda+i\sigma kl)\tilde{u}_\theta+(\lambda^2+\sigma k^2)\tilde{u}=0. \tag{19}$$

After the change of variable $\tilde{x}=\delta\theta$, substitution of the explicit expression for U from Eq. (16), and dropping the tildes, Eq. (19) reduces to

$$u_{xxxx}-4[(1-3\mathrm{sech}^2\,x)u]_{xx}-\gamma u_x+\beta u=0, \tag{20}$$

where

$$\gamma=\frac{2(c\lambda+i\sigma kl)}{\delta^3}\quad\text{and}\quad\beta=\frac{\lambda^2+\sigma k^2}{\delta^4}. \tag{21}$$

To obtain explicit solutions of this equation, we note that by taking $u=\phi_{xx}$ and $v=1-3\ \mathrm{sech}^2x$ in Eq. (20), and integrating twice the equation simplifies to

$$\phi_{xxxx}-4v\,\phi_{xx}-\gamma\phi_x+\beta\phi=0. \tag{22}$$

Solutions of this equation can be readily found in a manner similar to that in Ref. [21] (see also [11]). First we note that in the limit $x\to\pm\infty$, Eq. (22) reduces to

$$\phi_{xxxx}-4\phi_{xx}-\gamma\phi_x+\beta\phi=0. \tag{23}$$

Substituting now $\phi=e^{\mu x}\hat{\phi}$, one can see that μ satisfies the quartic equation

$$\mu^4-4\mu^2-\gamma\mu+\beta=0. \tag{24}$$

Quartics of this form have been analyzed in Ref. [5] [see Eq. (10.9) there], and when $\mathrm{Re}(\beta)>0$ there are two roots with positive real part and two roots with negative real part. Therefore, the space of solutions decaying as $x\to+\infty$ is two dimensional, as is the space of solutions decaying as $x\to-\infty$.

If the four roots μ_j, $j=1,\ldots,4$ of Eq. (24) are distinct, the corresponding solutions of Eq. (22) are given by

$$\phi_j(x)=e^{\mu_j x}h_j(x), \tag{25}$$

with

$$h_j(x)=(4\mu_j^3+8\mu_j-\gamma)-12\mu_j^2\tanh x. \tag{26}$$

The case of multiple roots can be handled similarly [21]. The solutions of the original equation (20) are found by substituting $u(x)=\phi(x)_{xx}$, and the other components of the vector $\mathbf{v}(x)$ can be obtained by differentiating the expression for $u(x)$.

Localized solutions of the linearized problem exist if one can match the solutions decaying as $x\to\infty$ with the solutions decaying as $x\to-\infty$. This can be determined by finding the zeros of the so-called Evans function, which correspond to the eigenvalues of the linearized problem. To define the Evans function, we write Eq. (20) as a first-order system

$$\mathbf{v}_x=A(x)\mathbf{v},\quad \mathbf{v}=\begin{pmatrix}u\\ u_x\\ u_{xx}\\ u_{xxx}\end{pmatrix},$$

$$A(x)=\begin{pmatrix}0 & 1 & 0 & 0\\ 0 & 0 & 1 & 0\\ 0 & 0 & 0 & 1\\ -\beta+4v_{xx} & \gamma+8v_x & 4v & 0\end{pmatrix} \tag{27}$$

with $v=1-3\ \mathrm{sech}^2\,x$.

Since the trace of the matrix $A(x)$ vanishes, the Evans function can be defined as $E(\lambda,k)=\mathbf{v}_1(x)\wedge\mathbf{v}_2(x)\wedge\mathbf{v}_3(x)\wedge\mathbf{v}_4(x)$ [22]. An alternative expression for the Evans func-

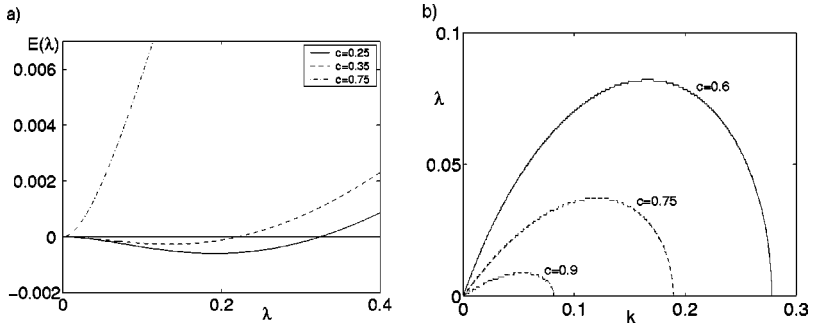

FIG. 2. (a) The Evans function $E(\lambda)=E(\lambda,0)$ versus λ for $c=0.25$, $c=0.35$, and $c=0.75$, respectively. (b) Growth rate versus transverse wave number for the values of velocity $c=0.6$, $c=0.75$, and $c=0.9$, respectively.

tion can be derived by using the adjoint system as shown in Ref. [23]. The adjoint system of Eq. (27) has the form

$$\mathbf{w}_x=-A(x)^*\mathbf{w}, \quad \mathbf{w}=\begin{pmatrix} w_1 \\ w_2 \\ w_3 \\ w_4 \end{pmatrix}, \tag{28}$$

where $A(x)^*$ denotes the Hermitian conjugate of A $[A(x)^*=\overline{A(x)^T}]$. The equation for w_4 turns out to be

$$(w_4)_{xxxx}-4v(w_4)_{xx}+\overline{\gamma}(w_4)_x+\overline{\beta}(w_4)=0. \tag{29}$$

This equation is equivalent to Eq. (22) up to the change of variables: $x\to -x$, $\gamma\to\overline{\gamma}$, $\beta\to\overline{\beta}$, and therefore its solutions can be obtained from Eq. (25) by changing x for $-x$ and conjugating them:

$$(w_4)_j=e^{-\mu_j^* x}\overline{h_j(-x)}, \tag{30}$$

with $h_j(x)$ defined in Eq. (26). Other components of the vector $\mathbf{w}(x)$ can be obtained from Eq. (28).

Let μ_1 and μ_2 be the two roots of Eq. (24) with negative real part, and let $\mathbf{v}_j(x)$ and $\mathbf{w}_j(x)$, $j=1,2$, be the corresponding solution vectors of the linearized (respectively, adjoint) system. Since the matrix $A(x)$ in Eq. (27) is traceless, we can define the Evans function for system (27) as follows [23]:

$$E(\lambda,k)=\begin{vmatrix} \langle \mathbf{w}_1(0),\mathbf{v}_1(0)\rangle & \langle \mathbf{w}_1(0),\mathbf{v}_2(0)\rangle \\ \langle \mathbf{w}_2(0),\mathbf{v}_1(0)\rangle & \langle \mathbf{w}_2(0),\mathbf{v}_2(0)\rangle \end{vmatrix}, \tag{31}$$

where $\langle\cdot,\cdot\rangle$ denotes the complex inner product in $\mathbb{C}^4$. To obtain a unique definition of the Evans function, the scaling $\lim_{x\to\infty} e^{-2\mu_j x}\langle \mathbf{w}_j(-x),\mathbf{v}_j(x)\rangle=1$ is used. This normalizes the eigenvectors and the adjoint eigenvectors of $A^\infty=\lim_{x\to\pm\infty}A(x)$.

After some lengthy algebra and introducing the scaling, which enforces the asymptotic limit $E(\lambda,k)\to 1$ as $\lambda\to\infty$, the final expression for the Evans function can be obtained, which we do not present here since it is lengthy (the expression for the Evans function as well as the calculations of the instability growth rate can be downloaded as a MAPLE file from the website [24]).

Zeros of the Evans function $E(\lambda,k)$ correspond to the bounded solutions of the linearized stability problem with the wave number k and the growth rate $\mathrm{Re}(\lambda)$. The leading order terms (in k and λ) in the Evans function are in complete agreement with the results of the geometric condition of Sec. III. Note that, since the construction here is based on a basic solitary wave with a nontrivial state at infinity, it is suggestive that the geometric condition [16] extends to such waves.

We illustrate the dependence of the Evans function on the wave speed and transverse wave number in Fig. 2. In the left graph, the transverse wave number is set to zero, to compare with the known results on longitudinal instability. The graph is in complete agreement with the known results (e.g., Refs. [3,5]) that the solitary wave is stable for $\frac{1}{2}<c\leqslant 1$ and unstable for $0\leqslant c<\frac{1}{2}$. In the right-hand graph in Fig. 2, we present the plot of the growth rate $\mathrm{Re}(\lambda)$ as a function of the transverse wave number. Note that the waves of the good Boussinesq which are longitudinally stable are transverse unstable. Note also that there is a cutoff wave number, similar to the other cases of the transverse instability, such as in the Zakharov-Kuznetsov equation [15].

V. POSTINSTABILITY SIMULATIONS

In this section, we perform a simulation of the PDE (1) using the multisymplectic spectral discretization proposed in Ref. [18] and applied there to Zakharov-Kuznetsov and shallow-water equations.

The $(2+1)$-dimensional Boussinesq equation is considered with $\varepsilon=D=-1$ on a finite domain $(x,y)=[0,L][0,L]$ with $L>0$ some constant, and periodic boundary conditions on both spatial variables. We choose a spatial mesh size as $\Delta x=\Delta y\equiv\Delta m=L/2N$ and introduce the discrete two-dimensional Fourier transform defined as

$$U_{kl}=\frac{1}{\sqrt{2N}}\sum_{i,j=1}^{2N} u_{ij}e^{-\theta_k(i-1)\Delta m-\theta_l(l-1)\Delta m},$$

where

$$\theta_k=i\frac{2\pi(k-1)}{L},$$

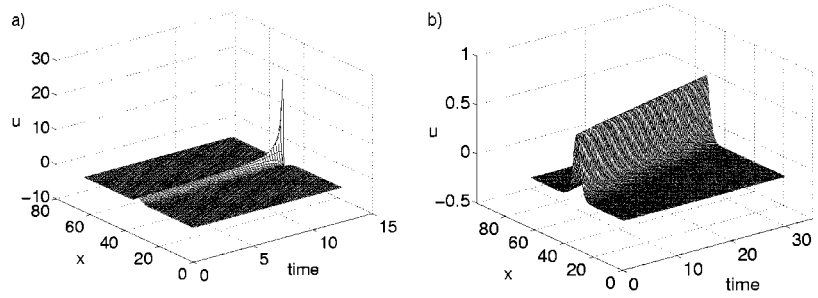

FIG. 3. (a) The development of the longitudinal instability and collapse at time $t=12.6$ for $c=\frac{1}{4}$. (b) Propagation of a stable solitary wave for $c=\frac{3}{4}$.

and $u_{ij}\approx u(m_{ij}), m_{ij}=(i-1)\Delta x+(j-1)\Delta y$ (cf. Ref. [25]). Fourier spectral discretization of the $(2+1)$-dimensional Boussinesq equation yields

$$\partial_{tt}U_{kl}=\overline{\theta}_k^2[\varepsilon\overline{\theta}_k^2U_{kl}+\nabla_{kl}\overline{F}(\mathbf{U})]+\sigma\overline{\theta}_l^2U_{kl}, \tag{32}$$

where $\overline{\theta}_k$ are the entries of the diagonal matrix defined by the relations

$$\overline{\theta}_k=\theta_k, \quad \text{for} \quad k=1,\ldots,N,$$

$\overline{\theta}_{N+1}=0$, and

$$\overline{\theta}_k=-\theta_{2N-k+2}, \quad \text{for} \quad k=N+2,\ldots,2N,$$

which follow from the periodicity of the discrete Fourier transform [25], and $\overline{F}(\mathbf{U})$ denotes the Fourier transform of the antiderivative of the function $f(u)$ in Eq. (1). The same result would be obtained if one applied the spectral discretization to the multisymplectic formulation (4), as it was done for the Zakharov-Kuznetsov equation in Ref. [18].

For the second-order time derivative we used the central difference approximation (time step was chosen to be $\Delta t=0.01$ in all the simulations):

$$\partial_{tt}U_{kl}=\frac{U_{kl}^{n+1}-2U_{kl}^n+U_{kl}^{n-1}}{\Delta t^2}. \tag{33}$$

One should note that the only valid test of this scheme can be done for the good Boussinesq equation with $\sigma>0$. For $\sigma<0$ in the case of the good Boussinesq equation, an initial profile independent of x would result in a solution which could grow "faster than exponential" because for large transverse wave numbers, the growth rate of the initial data has no upper bound (ill posedness).

To test the algorithm, we first used it to confirm the results for the dynamics of the one-dimensional solitary waves. The initial profile was taken to be of the form

$$u(x)=\frac{3}{2}(1-c^2)\mathrm{sech}^2\left[\frac{1}{2}(1-c^2)\left(x-\frac{L}{2}\right)\right]+\xi(x), \tag{34}$$

where $\xi(x)$ is a small random perturbation. The results are presented in Figs. 3 and 4. For $c=\frac{1}{4}$ the solitary wave solution is linearly unstable as reported in Refs. [4,5], and the development of this linear instability is shown in Fig. 3(a). In the case $c=\frac{3}{4}$ the numerical results confirm the stability of the solitary wave [see Fig. 3(b)]. The simulations were run on an interval of the length $L=64$ with $2N=128$. As a numerical check, the total energy determined by the Hamiltonian (2) was monitored, and it was found to be well behaved till near the collapse when the significant errors occur, as illustrated in Fig. 4.

For the two-dimensional simulations, we took an initial profile in the form of the line solitary wave uniform in y,

$$u(x,y,0)=\frac{3}{2}(1-c^2)\mathrm{sech}^2\left[\frac{1}{2}(1-c^2)\left(x-\frac{L}{2}\right)\right]+\xi(x,y), \tag{35}$$

where $\xi(x,y)$ is a small random perturbation (in this case $l=0$). In the case $c=\frac{1}{4}$, the solitary wave (35) is linearly unstable in longitudinal direction as is known from the stability analysis of the one-dimensional (1D) equation. In Fig.

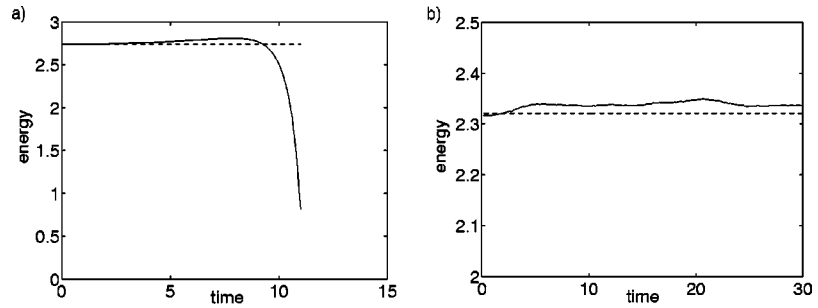

FIG. 4. Energy evolution. The dashed line represents the initial energy level, and the solid line shows the time evolution of energy. (a) Unstable case $c=\frac{1}{4}$. (b) Stable case $c=\frac{3}{4}$.

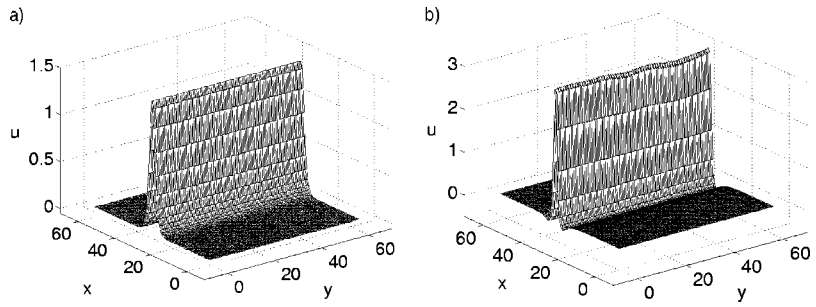

FIG. 5. Solitary wave for $\sigma=1$ and $c=\frac{1}{4}$. (a) Initial profile. (b) The development of the transverse modulation (time $t=11.25$).

5(b) we can see this instability developing in a similar way as in the 1D case. Wave collapse in this case is shown in Fig. 6(a), with the plot of energy as a function of time in Fig. 6(b). To illustrate that the instability is due to one-dimensional longitudinal effects, we present in Fig. 7 plots of the time evolution of the maximal amplitude of the solution, which behaves similarly in 1D and 2D cases.

When $c=\frac{3}{4}$, the solitary wave is longitudinally stable but transversely unstable, and the development of this instability is presented in Figs. 8 and 9. The length of the square box was chosen to be $L=128$ with the number of Fourier modes $2N=256$. If the perturbation added is of the form of a noise that is uniform in both directions, one can expect during time evolution a selection of the transverse wave number corresponding to the most unstable eigenmode as is illustrated in Fig. 8(b). Using a Fourier transform of the wave profile, we found in this case that the wave number selected is $k=0.123\pm0.003$, which is a good approximation of the wave number found from the analytical prediction $k_{max}=0.121$ [cf. Fig. 2(b)]. To further investigate the long-time dynamics and verify the analytically predicted growth rate, we start a computation with a perturbation proportional to $\cos(0.123y)$, which corresponds to the most unstable eigenmode. At the initial stage of the evolution transverse modulation has a slowly growing amplitude, and then the instability prevails leading finally to the collapse of the wave as shown in Fig. 9(a). The energy proves to be conserved rather well during the simulations [see Fig. 9(b)], although it deviates substantially as the wave approaches the stage of collapse.

The growth of the amplitude, followed by the fast collapse can be observed in Fig. 10(a). In order to compare the theoretical and numerical growth rates, we present in Fig. 10(b) the plot of $\ln\|u(t)-u(0)\|^2$ as a function of time. From the Fig. 10(a), we see that it takes some time for the transverse instability to develop. Therefore, we choose as a starting point for comparison a time interval when the most unstable eigenmode has already been selected by the solution, and one is still within the linear regime. It can be seen from Fig. 10(b) that the corresponding growth rate for the solution is close to the one determined by the most unstable eigenvalue (numerical value of the growth rate is $\lambda_{num}\approx0.0367$, while the analytical result is $\lambda_{anal}\approx0.0371$). For larger time nonlinear effects start playing a role, and they finally lead to the collapse.

VI. CONCLUDING REMARKS

We have considered the transverse instability of line solitary wave solutions of the $(2+1)$-dimensional Boussinesq equation. Using the multisymplectic formulation of the system, we derived a geometric condition for this instability for small transverse wave numbers. With an Evans function approach, the linearized stability equation was analyzed, and this allowed to obtain the dependence of the instability growth rate for all transverse wave numbers. Numerical simulations support the analytical predictions about transverse and longitudinal instabilities and demonstrate the development of those instabilities and subsequent wave collapse. Analytical and numerical conclusions about the wave number and the growth rate corresponding to the most unstable eigenmode are also in good agreement.

We conclude with an open problem. While analytic theories for the collapse of solitary waves for the Boussinesq equation in one space dimension exist [19], it is an interest-

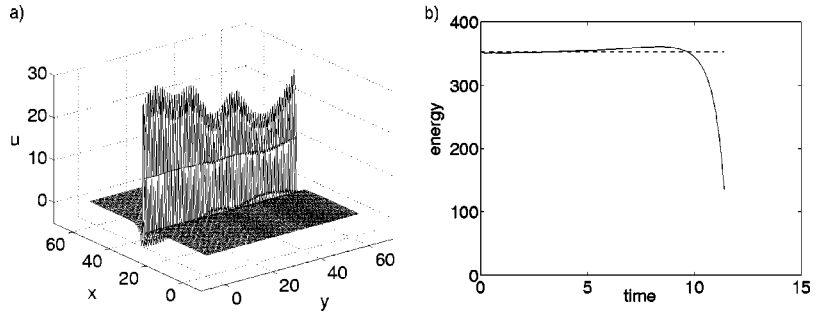

FIG. 6. The same as in Fig. 5. (a) Wave collapse (time $t=12.6$). (b) Energy evolution. The dashed line represents the initial energy level, and the solid line shows the time evolution of energy.

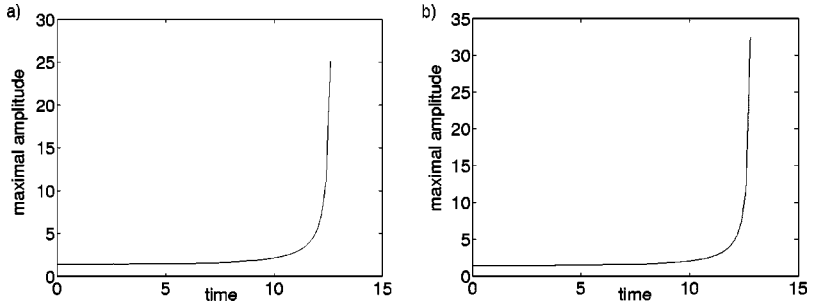

FIG. 7. Time evolution of the maximal amplitude for the 1D unstable solution with $c=\frac{1}{4}$. (a) One-dimensional case. (b) Two-dimensional case.

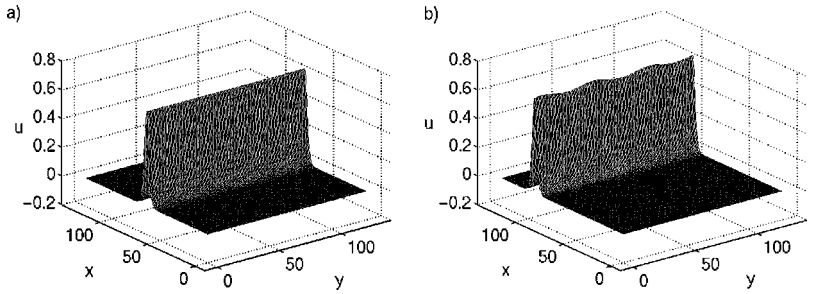

FIG. 8. Solitary wave for $\sigma=1$ and $c=\frac{3}{4}$. (a) Initial profile. (b) The development of the transverse modulation (time $t=210$).

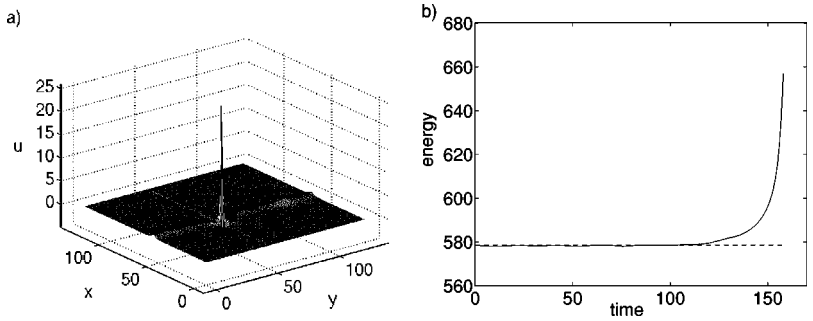

FIG. 9. The same as in Fig. 8. (a) Wave collapse after transverse modulation (time $t=159$). (b) Energy evolution. The dashed line represents the initial energy level, and the solid line shows the time evolution of energy.

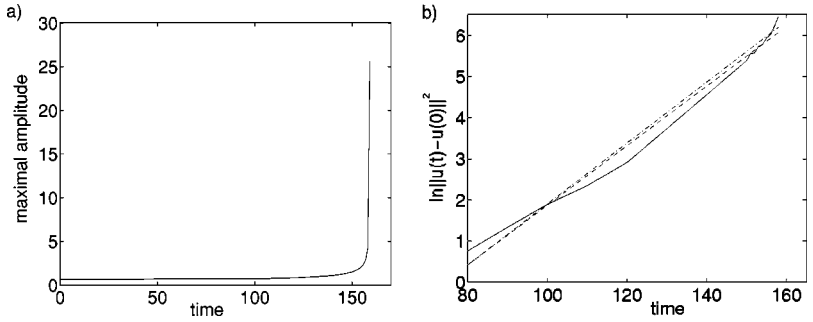

FIG. 10. (a) The time evolution of the maximal amplitude for the transversely unstable solution with $c=\frac{3}{4}$. (b) The evolution of $\ln\|u(t)-u(0)\|^2$. The solid line represents the actual solution, the dashed line corresponds to its linear approximation, and the dash-dotted line is the line of the maximal analytical growth rate.

ing open problem to develop an analytical technique for predicting collapse for the case of two space dimensions, e.g., a generalization of the virial theorem or the result of Ref. [19], for example, and moreover, to determine if the transverse instability for Eq. (1) leads to the collapse for *all* parameter values.

ACKNOWLEDGMENTS

The authors would like to thank Sebastian Reich for advice on the numerics and Georg Gottwald for helpful discussions.

[1] R.S. Johnson, J. Fluid Mech. **323**, 65 (1996).
[2] B.N. Breizman, and V.M. Malkin, Sov. Phys. JETP **52**, 435 (1980).
[3] J.L. Bona, and R.L. Sachs, Commun. Math. Phys. **118**, 15 (1988).
[4] J.C. Alexander, and R.L. Sachs, Nonlinear World **2**, 471 (1995).
[5] T.J. Bridges, and G. Derks, Arch. Ration. Mech. Anal. **156**, 1 (2001).
[6] V.E. Zakharov, Sov. Phys. JETP **26**, 994 (1968).
[7] B.B. Kadomtsev, and V.I. Petviashvili, Appl. Phys. **15**, 539 (1970).
[8] E.A. Kuznetsov, A.M. Rubenchik, and V.E. Zakharov, Phys. Rep. **142**, 104 (1986).
[9] E.W. Laedke, and K.H. Spatschek, Phys. Rev. Lett. **41**, 1798 (1978).
[10] X.P. Wang, M.J. Ablowitz, and H. Segur, Physica D **78**, 241 (1994).
[11] J.C. Alexander, R.L. Pego, and R.L. Sachs, Phys. Lett. A **226**, 187 (1997).
[12] M.A. Allen, and G. Rowlands, Phys. Lett. A **235**, 145 (1997).
[13] E. Infeld, G. Rowlands, and A. Senatorski, Proc. R. Soc. London, Ser. A **455**, 4363 (1999).
[14] Y.S. Kivshar, and D.E. Pelinovsky, Phys. Rep. **331**, 117 (2000).
[15] M.A. Allen, and G. Rowlands, J. Plasma Phys. **50**, 413 (1993).
[16] T.J. Bridges, Phys. Rev. Lett. **84**, 2614 (2000).
[17] T.J. Bridges, J. Fluid Mech. **439**, 255 (2001).
[18] T.J. Bridges, and S. Reich, Physica D **152-153**, 491 (2001).
[19] S.K. Turitsyn, Phys. Rev. E **47**, R796 (1993).
[20] T. J. Bridges and G. Derks (unpublished).
[21] J.G. Berryman, Phys. Fluids **19**, 771 (1976).
[22] J.C. Alexander, Gardner, R., and C.K.R.T. Jones, J. Nanosci. Nanotechnol. **410**, 167 (1990).
[23] T.J. Bridges, and G. Derks, Phys. Lett. A **251**, 363 (1999).
[24] K.B. Blyuss, http://www.maths.surrey.ac.uk/personal/pg/K.Blyuss/
[25] B. Fornberg, *A Practical Guide to Peudospectral Methods* (Cambridge University Press, Cambridge, 1996).